Stability Analysis of I-Pδ Controllers for SISO Time-Delay Systems

Julián-Alejandro Hernández-Gallardo[1,2], Silviu-Iulian Niculescu[3],
César-Fernando Méndez-Barrios[1] and E. Moreno-Negrete[1,2]

Abstract— **This paper addresses the stability analysis of closed-loop linear single-input single-output (SISO) systems equipped with a low-complexity I-Pδ controller. The proposed structure, which incorporates integral action, a proportional gain, and a delayed output feedback term, is presented as a robust alternative to classical PID and I-PD schemes. By replacing the derivative action with a delayed term, the controller avoids amplifying high-frequency measurement noise while preserving the damping injection of its PID counterpart. The stability analysis is performed in the parameter space of the controller gains, for which analytical expressions of the stability crossing boundaries are derived. Practical guidelines for selecting the controller parameters are established, and the approach's effectiveness is demonstrated through numerical examples, highlighting its superior performance in noisy environments compared to derivative-based structures.**

I. Introduction

Proportional-Integral-Derivative (PID) controllers remain the cornerstone of industrial automation owing to their structural simplicity, satisfactory performance across a wide range of applications, and the intuitive physical interpretation of their parameters [1], [2]. Despite their widespread success, the implementation of the derivative (D) action continues to present significant practical challenges, particularly in systems affected by high-frequency measurement noise [3]. Since differentiation inherently amplifies high-frequency components, the derivative term may generate excessive control activity, accelerate actuator wear, and, in severe cases, compromise closed-loop performance and robustness.

To alleviate these drawbacks, several modified PID architectures have been proposed, among which the I-PD and PI-D structures are perhaps the most representative [4], [5]. By relocating the derivative action to the feedback path, these configurations successfully eliminate the well-known derivative-kick phenomenon associated with abrupt set-point variations [6]. Nevertheless, the intrinsic sensitivity of the derivative action to measurement noise remains largely unchanged. As a consequence, practical implementations typically rely on additional low-pass filtering stages. Although effective in attenuating noise, these filters increase the controller order, introduce extra tuning parameters, and modify the closed-loop dynamics in ways that are often neglected during the design stage.

These limitations have motivated the search for alternative mechanisms capable of providing the damping and phase-lead effects traditionally associated with derivative control, while avoiding its inherent sensitivity to noise. In this context, delay-based control strategies have emerged as a promising alternative. As shown in [7], [8], intentionally introduced delays can be exploited as additional design parameters rather than being regarded solely as sources of performance degradation or instability. In particular, a delayed proportional feedback term of the form $k_\delta y(t-h)$ can reproduce several beneficial effects commonly associated with derivative action. Unlike an ideal differentiator, however, delayed feedback does not amplify high-frequency measurement noise and naturally exhibits low-pass filtering characteristics, while still contributing the phase lead and damping injection required to improve transient performance and stabilize challenging dynamical systems.

Motivated by this observation, this paper focuses on the I-Pδ controller, a low-complexity structure obtained by replacing the derivative term of an I-PD controller with a delayed output feedback. The underlying idea is illustrated in Fig. 1, where the closed-loop responses and control signals of a conventional I-PD controller and the proposed I-Pδ scheme are compared under noisy measurements. As can be observed, both controllers are able to achieve comparable tracking performance. However, the I-Pδ controller produces a significantly smoother control signal, revealing its ability to preserve a derivative-like damping effect while attenuating the impact of measurement noise.

Although this motivating example highlights the practical advantages of the I-Pδ structure, a systematic tuning procedure requires a precise characterization of the closed-loop stability region. This is the main objective of the present work. More specifically, we address the stability analysis of linear time-invariant single-input single-output systems controlled by an I-Pδ scheme. By employing a geometric approach in the (k_p, k_i, k_δ) parameter space, analytical expressions for the stability crossing boundaries are derived. These boundaries allow us to characterize the regions where stability switches occur and provide practical guidelines for selecting the controller gains and the delay parameter h.

The main contribution of this paper is therefore twofold. First, it establishes a formal parameter-space characterization of the stability regions induced by the I-Pδ controller. Second, it shows how this characterization can be used as a systematic tuning framework for obtaining low-complexity

[1] Universidad Autónoma de San Luis Potosí (UASLP), Facultad de Ingeniería, Dr. Manuel Nava No. 8, Zona Universitaria, San Luis Potosí, S.L.P., México. julian_@ieee.org, fernando.barrios@uaslp.mx

[2] Departamento de Ingeniería, Tecnológico Salesiano Carlos Gómez, J. Venegas No. 5, Virreyes, C.P, 78240 San Luis Potosí, SLP, Mexico.

[3] Université Paris-Saclay, CNRS, CentraleSupélec, Inria, Laboratoire des Signaux et Systèmes (L2S, UMR CNRS 8506), F-91192, Gif-sur-Yvette, France.

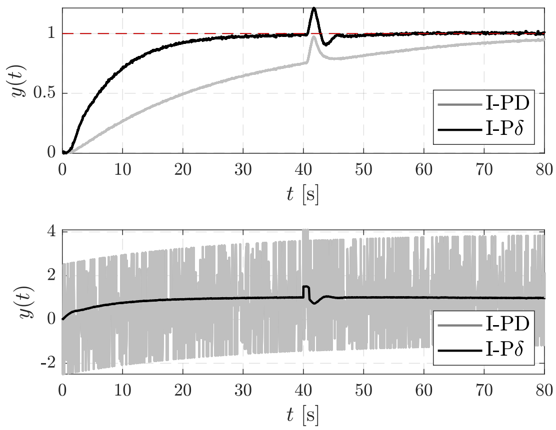

Fig. 1: Time responses and control signals for the I-PD and I-Pδ controllers under noisy measurements.

controllers that retain the damping benefits of derivative-based structures while improving robustness against high-frequency measurement noise.

The rest of the paper is organized as follows. Section II presents the system description and the I-Pδ controller structure. Section III develops the geometric stability analysis and derives the corresponding stability crossing boundaries. Numerical results and comparisons with derivative-based structures are provided in Section IV. Finally, concluding remarks are presented in Section V.

The following standard notation is adopted throughout the paper. The sets of real, strictly positive real, and strictly negative real numbers are denoted by $\mathbb{R}$, $\mathbb{R}_+$, and $\mathbb{R}_-$, respectively. $\mathbb{C}$ denotes the set of complex numbers. The imaginary unit is denoted by $\boldsymbol{i} := \sqrt{-1}$. For $z = \sigma \pm \boldsymbol{i}\omega$, with $\sigma, \omega \in \mathbb{R}$, the symbols $\bar{z}$, $\Re(z)$, and $\Im(z)$ denote the complex conjugate, real part, and imaginary part of z, respectively.

II. Problem Formulation

Consider the class of strictly proper linear time-invariant (LTI) single-input single-output (SISO) plants with an input-output delay, described by the transfer function

$$G(s) = \frac{P(s)}{Q(s)} e^{-\tau s}, \tag{1}$$

where $P(s)$ and $Q(s)$ are polynomials with real coefficients, and $\tau \geq 0$ denotes the inherent delay of the plant. Throughout the paper, the following regularity assumptions are considered.

Assumptions 1: The plant $G(s)$ satisfies the following structural properties:

(i) $G(s)$ is strictly proper $(\deg(Q(s)) > \deg(P(s)))$.
(ii) $P(s)$ and $Q(s)$ are coprime polynomials.
(iii) $P(\boldsymbol{i}\omega) \neq 0$ for all $\omega \in \mathbb{R}$.

Assumption 1-(i) is imposed to ensure a well-posed closed-loop interconnection and, in conjunction with the proposed controller structure, to obtain a characteristic equation of retarded type. This property is essential for the subsequent stability analysis, since retarded quasipolynomials have only a finite number of roots in any closed right half-plane. Assumption 1-(ii) excludes pole-zero cancellations, so that the characteristic equation obtained from the input-output description captures the relevant closed-loop dynamics. Finally, Assumption 1-(iii) avoids singular cases on the imaginary axis.

Problem 1: Given the plant (1) satisfying Assumption 1, determine the set of controller parameters for which the closed-loop system is asymptotically stable when controlled by an I-Pδ scheme. In particular, characterize the stability regions in the (k_p, k_i, k_δ) parameter space for a prescribed induced delay $h > 0$ and plant delay $\tau \geq 0$.

The I-Pδ control architecture considered in this work is shown in Fig. 2. The integral action is placed in the forward path to ensure zero steady-state error for constant references, whereas the proportional and delayed output feedback terms are implemented in the feedback path. This structure is inspired by the classical I-PD configuration, but replaces the derivative action with a delayed proportional term. In this way, the controller aims to retain derivative-like damping and phase-lead effects while avoiding the direct amplification of high-frequency measurement noise.

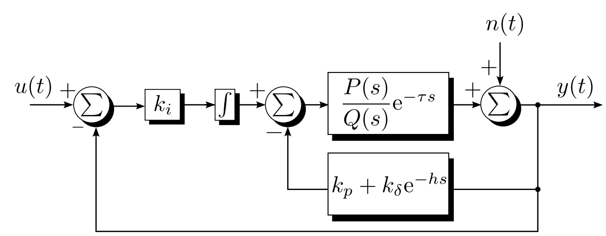

Fig. 2: Closed-loop control scheme with the I-Pδ structure.

The corresponding control law is given by

$$u(t) = k_i \int_0^t e(r)dr - k_p y(t) - k_\delta y(t-h), \tag{2}$$

where $e(t) = r(t) - y(t)$ denotes the tracking error, $\boldsymbol{k} = (k_p, k_i, k_\delta)$ is the vector of controller gains, and $h > 0$ is the intentionally introduced delay. The gains k_p, k_i, and k_δ correspond, respectively, to the proportional feedback, integral, and delayed feedback actions.

By taking the Laplace transform of (2) and considering the closed-loop interconnection in Fig. 2, we obtain the closed-loop characteristic function

$$\Delta(s; \boldsymbol{k}, h, \tau) \triangleq sQ(s) + \left(k_i + s\left(k_p + k_\delta e^{-hs}\right)\right) P(s) e^{-\tau s}. \tag{3}$$

Under Assumption 1, the characteristic equation

$$\Delta(s; \boldsymbol{k}, h, \tau) = 0 \tag{4}$$

is of retarded type. Therefore, closed-loop stability is determined by the location of the roots of (3). The next section develops a geometric stability analysis aimed at characterizing the crossing boundaries in the controller-parameter space.

III. Stability Crossing Characterization

In this section, we characterize the stability regions in the (k_p, k_i, k_δ) parameter space by identifying the boundaries where characteristic roots cross the imaginary axis.

The following definitions will be of core importance in the development of our main results.

Definition 1 (Frequency Crossing Set): The *frequency crossing set* $\Omega \subset \mathbb{R}_+ \cup \{0\}$ is defined as the set of all frequencies ω for which there exists at least one triple (k_p, k_i, k_δ) with a fixed delay h such that the characteristic equation (3) has a root $s = \boldsymbol{i}\omega$. Due to the symmetry of the quasipolynomial's roots, we restrict our analysis to nonnegative frequencies.

A. Characterization of the Stability Boundaries

The boundary $\mathcal{T}$ of the stability region in the parameter space is composed of the *real root boundary* (RRB), denoted by $\mathcal{T}_0$, and the *complex root boundary* (CRB), denoted by $\mathcal{T}_\omega$, i.e.,

$$\mathcal{T} = \mathcal{T}_0 \cup \mathcal{T}_\omega.$$

The following propositions provide explicit formulae to construct these hypersurfaces.

Proposition 1 (Real Root Boundary $\mathcal{T}_0$): Let $h, \tau \in \mathbb{R}_+$ be fixed delays. Then, the real root boundary $\mathcal{T}_0 \subset \mathbb{R}^3$ is defined as the set of all parameters (k_p, k_i, k_δ) for which the characteristic equation (3) has a root at $s = 0$. This set is given by the plane

$$\mathcal{T}_0 := \left\{ (k_p, k_i, k_\delta) \in \mathbb{R}^3 \;\middle|\; k_i = 0, \;\; k_p = -\frac{Q(0)}{P(0)} - k_\delta \right\}, \tag{5}$$

where $P(s)$ and $Q(s)$ are given in (1). The set $\mathcal{T}_0$ defines a stability crossing curve corresponding to a crossing through the origin of the complex plane.

Proof: Substituting $s = 0$ into (3) yields $0 \cdot Q(0) + (k_i + 0 \cdot (k_p + k_\delta))P(0) \cdot 1 = k_i P(0) = 0$. Since $P(0) \neq 0$ by Assumption 1-(iii), we obtain $k_i = 0$. The condition $k_p + k_\delta = -Q(0)/P(0)$ follows from the steady-state requirement $\lim_{s\to 0} s^{-1}\Delta(s) = 0$, which ensures the integral action eliminates the steady-state error. Hence, $\mathcal{T}_0$ is exactly the plane described in (5). ■

Proposition 2 (Complex Root Boundary $\mathcal{T}_\omega$): Let $h, \tau \in \mathbb{R}_+$ be fixed delays. Assume that $\omega \in \Omega$ satisfies $\omega \neq n\pi/h$ for $n \in \mathbb{N}$. Then, the complex root boundary $\mathcal{T}_\omega \subset \mathbb{R}^3$ is defined as the set of all parameters (k_p, k_i, k_δ) for which the characteristic equation (3) has a pair of purely imaginary roots $s = \pm\boldsymbol{i}\omega$. This set is given by

$$\mathcal{T}_\omega := \bigcup_{\omega\in\Omega} \left\{ \boldsymbol{k} \in \mathbb{R}^3 \;\middle|\; \begin{array}{l} k_i = \mathcal{R}(\omega) - \omega \sin(h\omega)\, k_\delta, \\ k_p = \dfrac{\mathcal{I}(\omega)}{\omega} - \cos(h\omega)\, k_\delta, \quad k_\delta \in \mathbb{R} \end{array} \right\},$$

where the frequency-dependent functions $\mathcal{R}(\omega)$ and $\mathcal{I}(\omega)$ are defined as

$$\begin{aligned} \mathcal{R}(\omega) &:= \Re\left\{ -\boldsymbol{i}\omega \frac{Q(\boldsymbol{i}\omega)}{P(\boldsymbol{i}\omega)} e^{\boldsymbol{i}\tau\omega} \right\}, \\ \mathcal{I}(\omega) &:= \Im\left\{ -\boldsymbol{i}\omega \frac{Q(\boldsymbol{i}\omega)}{P(\boldsymbol{i}\omega)} e^{\boldsymbol{i}\tau\omega} \right\}. \end{aligned}$$

Proof: Setting $s = \boldsymbol{i}\omega$ in (3) and multiplying by $e^{\boldsymbol{i}\tau\omega}$ (which is nonzero) gives

$$k_i + \boldsymbol{i}\omega k_p + \boldsymbol{i}\omega k_\delta e^{-\boldsymbol{i}h\omega} = -\boldsymbol{i}\omega \frac{Q(\boldsymbol{i}\omega)}{P(\boldsymbol{i}\omega)} e^{\boldsymbol{i}\tau\omega}.$$

Define $H(\boldsymbol{i}\omega) := -\boldsymbol{i}\omega \dfrac{Q(\boldsymbol{i}\omega)}{P(\boldsymbol{i}\omega)} e^{\boldsymbol{i}\tau\omega} = \mathcal{R}(\omega) + \boldsymbol{i}\mathcal{I}(\omega)$. Using $e^{-\boldsymbol{i}h\omega} = \cos(h\omega) - \boldsymbol{i}\sin(h\omega)$ and equating real and imaginary parts yields the linear system

$$\begin{cases} k_i + \omega \sin(h\omega) k_\delta = \mathcal{R}(\omega), \\ \omega k_p + \omega \cos(h\omega) k_\delta = \mathcal{I}(\omega). \end{cases}$$

Solving for k_i and k_p directly leads to the parametric description of $\mathcal{T}_\omega$ given above. The union over all $\omega \in \Omega$ collects all possible crossing frequencies. ■

Remark 1: For each fixed ω, the set $\mathcal{T}_\omega$ describes a line in the (k_p, k_i)-plane parameterized by k_δ. The complete complex root boundary $\mathcal{T}_\omega$ is therefore a ruled surface in $\mathbb{R}^3$ obtained by sweeping ω over Ω. This geometric interpretation is essential for the subsequent stability analysis.

Remark 2: The total stability crossing set is $\mathcal{T} = \mathcal{T}_0 \cup \mathcal{T}_\omega$. The number of unstable roots of the characteristic equation remains invariant in each connected component of $\mathbb{R}^3 \setminus \mathcal{T}$, which forms the basis for the stability region determination.

B. σ-stability

To impose an additional desired degree of exponential stability, the variable transformation $s \to s - \sigma$ is introduced, which is known as σ-stability. This reformulation allows the stability analysis to be performed with respect to a shifted complex plane, making it possible to determine the sets of controller parameters for which all roots of the closed-loop system characteristic lie to the left of the vertical line $\Im(s)$.

Definition 2 (Spectral abscissa): The spectral abscissa of the system, denoted by $\rho(\Delta)$, is defined as the largest real part among all the roots of the characteristic equation $\Delta(s)$. That is,

$$\rho(\Delta) := \max\left\{ \Re\{s\} : \Delta(s; \boldsymbol{k}, h, \tau) = 0, \; s \in \mathbb{C} \right\}. \tag{6}$$

Definition 3 ($\sigma-$stability): For a given $\sigma > 0$, the quasi-polynomial $\Delta(s; \boldsymbol{k}, h, \tau)$ is said to be σ-stable whenever all its roots lie in the half-plane $\Re(s) \leq -\sigma$, that is,

$$\rho(\Delta) \leq -\sigma. \tag{7}$$

To study the σ-stability of the system, it is necessary to examine the roots located on the shifted imaginary axis, given by $s = -\sigma \pm \boldsymbol{i}\omega$, for a prescribed triplet (k_p, k_i, k_δ). In this setting, let $\mathcal{T}_\sigma$ denote the set of controller parameters $\boldsymbol{k}$ for which the quasi-polynomial (3) admits at least one root on the vertical line

$$\boldsymbol{L}_\sigma := \{ s \in \mathbb{C} \mid s = -\sigma + \boldsymbol{i}\omega, \; \omega \in \mathbb{R} \}.$$

Throughout the remainder of this section, this line will be referred to as the σ-axis.

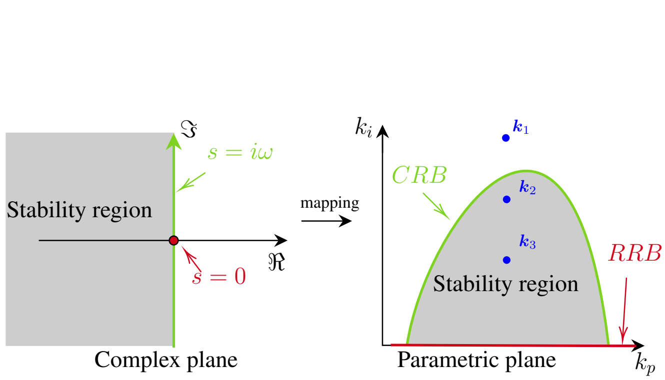

(a) Mapping of the stability crossing boundaries from the complex $s-$plane to the $(k_p, k_i)-$parametric plane.

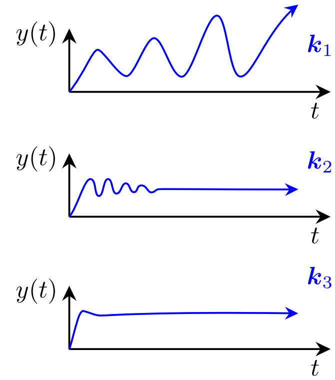

(b) Time responses of the closed-loop system under different sets of (k_p, k_i) gains.

Fig. 3: Stability analysis and time-domain performance of the closed-loop system for different controller parameters.

Proposition 3: The stability crossing boundaries associated to (3) are described with $\sigma \in \mathbb{R}_+$ defined in (8)

$$\begin{aligned} k_i(\omega, \sigma, k_\delta, h) &:= \frac{1}{\omega}\Big[\sigma\, \Im\left\{(\sigma - \boldsymbol{i}\omega)\; G(\boldsymbol{i}\omega - \sigma)^{-1}\right\} \\ &\quad + \omega\, \Re\left\{(\sigma - \boldsymbol{i}\omega)\; G(\boldsymbol{i}\omega - \sigma)^{-1}\right\} \\ &\quad - \mathrm{e}^{\sigma h}\left(\sigma^2 + \omega^2\right) \sin\left(\omega h\right) k_\delta\Big], \\ k_p(\omega, \sigma, k_\delta, h) &:= \frac{1}{\omega}\Big[\Im\left\{(\sigma - \boldsymbol{i}\omega)\; G(\boldsymbol{i}\omega - \sigma)^{-1}\right\} \\ &\quad - \mathrm{e}^{\sigma h}\left(\omega \cos\left(\omega h\right) + \sigma \sin\left(\omega h\right)\right) k_\delta\Big], \end{aligned} \tag{8}$$

con $\omega = 0$ defined in (9)

$$\begin{aligned} k_i(\sigma, k_p, k_\delta) &:= \sigma\Big[G(-\sigma)^{-1}\, \mathrm{e}^{-\tau\sigma} + k_p + k_\delta \mathrm{e}^{h\sigma}\Big], \\ k_p &\in \mathbb{R}, \end{aligned} \tag{9}$$

where the term $G(\cdot)^{-1}$ is defined by $G(\xi)^{-1} = \dfrac{Q(\xi)}{P(\xi)} e^{\tau\xi}$.

IV. Numerical Examples

This section illustrates the proposed I-Pδ stability framework through three case studies: a first-order DC motor model, an unstable non-minimum phase system, and a higher-order plant. For each example, stability regions are computed for $h_1 = 0.01$ s and $h_2 = 0.5$ s, while closed-loop performance is assessed using unit step references and constant disturbances of magnitude ± 0.5 applied at $t_1 = 40$ s and $t_2 = 80$ s.

A. Example 1: DC Motor Velocity Control (First-Order)

Consider the following first-order transfer function, representing the relationship between input voltage and angular velocity of a DC motor [9]:

$$G\left(s\right) = \frac{1.0646 e^{-0.084 s}}{0.056 s + 1}. \tag{10}$$

The stability regions are depicted in Fig. 4. A comparison between Figs. 4a and 4b clearly shows that increasing the delay h significantly reshapes the stability surface. Specifically, as the delay increases from $h = 0.01$ s to $h = 0.5$ s, the stability surface shrinks, thereby making the tuning process more restrictive.

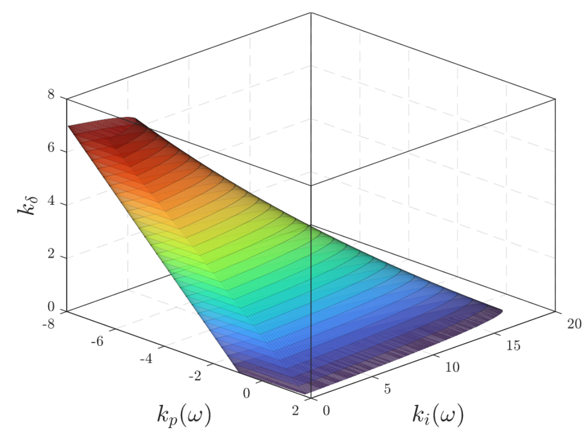

(a) $h = 0.01$ s.

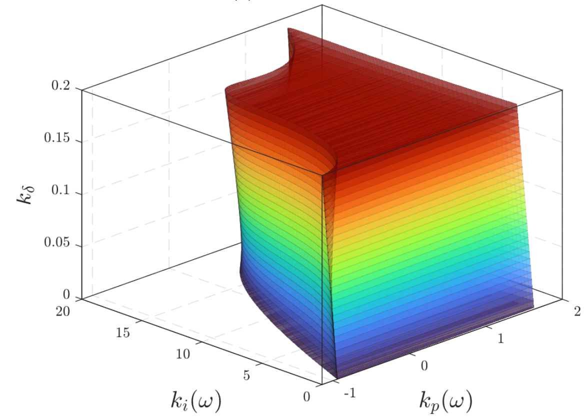

(b) $h = 0.5$ s.

Fig. 4: Stability region for the system (10).

A controller is selected with $(k_p, k_i, k_\delta, h) = (-0.9221, 0.5499, 0.4746, 0.01)$. The corresponding closed-loop response is shown in Fig. 5, demonstrating effective regulation and disturbance rejection.

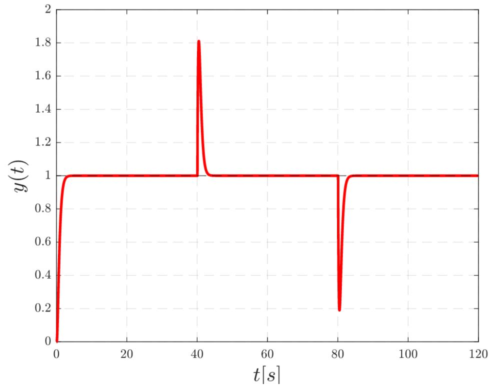

Fig. 5: Time response for I-Pδ controller with $h = 0.01$ s (Example 1).

B. Example 2: Unstable Non-Minimum Phase System (Second-Order)

Consider the following second-order, non-minimum-phase, unstable plant (borrowed from [10], [11]):

$$G_1(s) = \frac{s-2}{s^2 - \frac{1}{2}s + \frac{13}{4}} e^{-2s}. \tag{11}$$

The open-loop system is unstable with poles at $s_{1,2} = 0.25 \pm \boldsymbol{i}1.785$. The stability regions are depicted in Fig. 6.

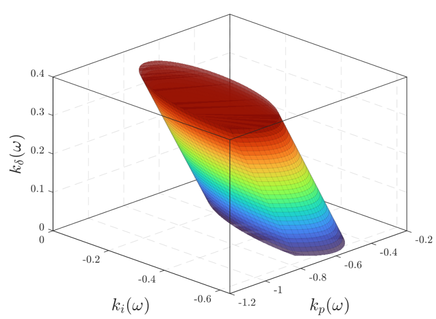

(a) $h = 0.01$ s.

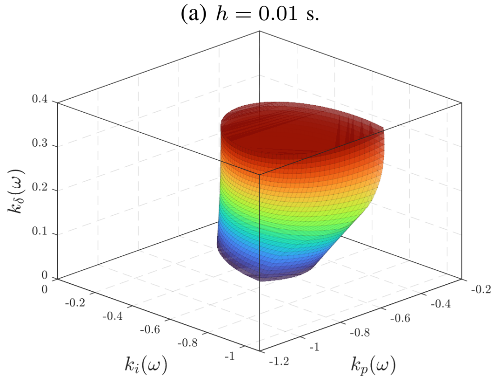

(b) $h = 0.5$ s.

Fig. 6: Stability regions for the system (11).

To improve the convergence decay rate of the system response, Proposition 3 is now considered. Its application is illustrated through two different cases, starting with the situation in which the delay is fixed at $h = 0.01$ s. As can be seen from both figures, the shape of the stability region may change.

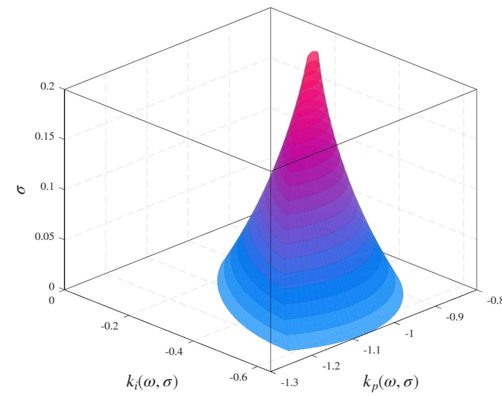

Fig. 7: (k_p, k_i)-plane for $(k_\delta, h) = (0.5, 0.01)$.

As σ increases, the admissible stability region shrinks, meaning that fewer controllers guarantee a higher prescribed decay rate. Hence, gains selected inside the regions shown in Fig. 7 shift the dominant closed-loop roots further to the left of the complex plane, producing faster transient responses. This behavior is illustrated using two stabilizing controllers, namely $(k_p, k_i, k_\delta, h) = (-0.58, -0.25, 0.15, 0.01)$ and $(-0.75, -0.75, 0.35, 0.5)$, whose responses are shown in Figs. 8 and 9, respectively. The results confirm that the larger induced delay improves the damping of the oscillatory response when compared with the small-delay, quasi-derivative case.

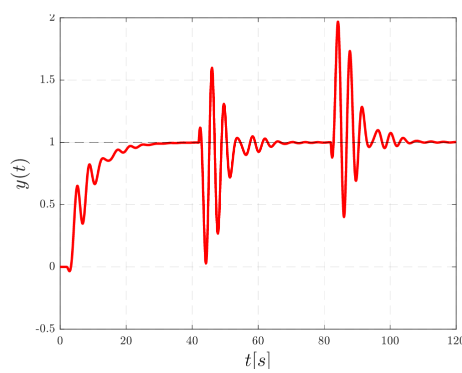

Fig. 8: Time response for I-Pδ controller (Example 2).

As this process continues, a limiting value is eventually reached, commonly referred to as the maximum σ. This corresponds to the real value of σ for which the stability region collapses into a single point. At this stage, the dominant poles cannot be assigned further to the left, meaning that no additional improvement in the exponential decay rate can be achieved within the proposed controller structure. Hence, this point represents the best achievable convergence rate for the closed-loop system under the considered control law.

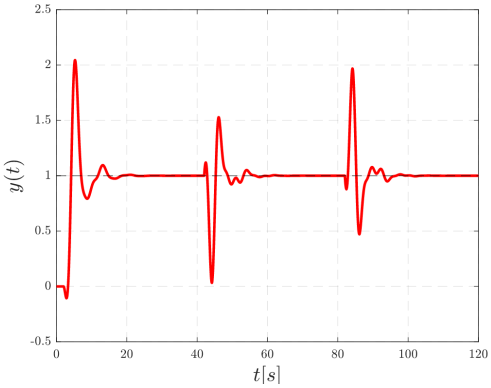

Fig. 9: Time response for I-Pδ controller (Example 2).

C. Example 3: High-Order Process (Sixth-Order)

Finally, we consider a sixth-order plant to demonstrate the scalability of the method [12]:

$$G_2(s) = \frac{-s^4 - 7s^3 - 2s + 1}{(s+1)(s+2)(s+3)(s+4)(s^2+s+1)} \mathrm{e}^{-\frac{1}{20}s}. \tag{12}$$

The stability regions are shown in Fig. 10. For $h = 0.01$ s (Fig. 10a), the surface is nearly planar and predictable. In contrast, for $h = 0.5$ s (Fig. 10b), the geometry becomes twisted, especially along the k_i direction, which directly impacts the distribution of feasible gains.

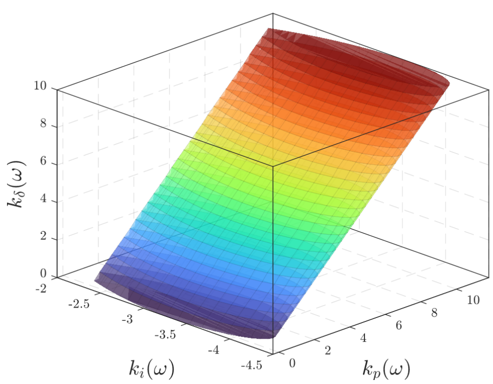

(a) $h = 0.01$ s.

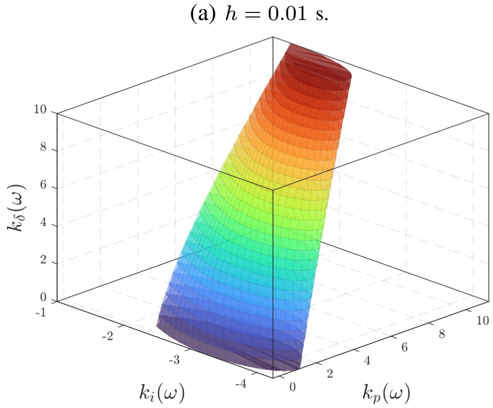

(b) $h = 0.5$ s.

Fig. 10: Stability regions for the system (12).

V. Concluding Remarks

This paper presented a geometric stability analysis for SISO time-delay systems controlled by an I-Pδ scheme. By replacing the derivative action of the classical I-PD controller with a delayed output feedback term, the proposed structure provides a low-complexity alternative that preserves derivative-like damping effects while reducing the amplification of high-frequency measurement noise.

Analytical expressions for the stability crossing boundaries were derived in the (k_p, k_i, k_δ) parameter space, for fixed plant and controller delays. These expressions provide a constructive way to identify stabilizing regions and to guide the controller tuning process. Numerical examples illustrated the applicability of the approach and showed how the induced delay modifies both the geometry of the stability regions and the resulting closed-loop behavior. Future work will address performance-oriented tuning rules, delay selection, and robustness extensions.

Acknowledgments

The work of C.-F. Méndez-Barrios has been supported by CONAHCyT–México, under the grant *Ciencia Básica y de Frontera:* CBF2023–2024–2696.

References

[1] T. Hagglund and K. J. Astrom, "PID controllers: theory, design, and tuning," *The Instrumentation, Systems, and Automation Soc.*, 1995.

[2] K. J. Åström and T. Hägglund, "The future of PID control," *Control engineering practice*, vol. 9, no. 11, pp. 1163–1175, 2001.

[3] C.-F. Méndez-Barrios, S.-I. Niculescu, A. Martínez-González, and A. Ramírez, "Characterizing some improperly posed problems in proportional-derivative control," *International Journal of Robust and Nonlinear Control*, vol. 32, no. 18, pp. 9452–9474, 2022.

[4] I. Kaya, "A PI-PD controller design for control of unstable and integrating processes," *ISA transactions*, vol. 42, no. 1, pp. 111–121, 2003.

[5] M. M. Ozyetkin, C. Onat, and N. Tan, "Pi-pd controller design for time delay systems via the weighted geometrical center method," *Asian Journal of Control*, vol. 22, no. 5, pp. 1811–1826, 2020.

[6] A. O'dwyer, *Handbook of PI and PID controller tuning rules*. World Scientific, 2009.

[7] J.-E. Hernández-Díez, C.-F. Méndez-Barrios, S. Mondié, S.-I. Niculescu, and E. González-Galván, "Proportional-delayed controllers design for LTI-systems: a geometric approach," *International Journal of Control*, vol. 91, no. 4, pp. 907–925, 2018.

[8] J.-A. Hernández-Gallardo, E. Moreno-Negrete, C. E. Garcia Cena, E. J. González-Galván, L. Félix, J. Á. Barrios, and C.-F. Méndez-Barrios, "A Synergistic Approach to Velocity Control under Intentional and Inherent Time Delays," in *2025 11th International Conference on Control, Decision and Information Technologies (CoDIT)*, vol. 1, pp. 297–302, IEEE, 2025.

[9] J.-A. Hernández-Gallardo, E.-J. González-Galván, C.-F. Méndez-Barrios, and A.-J. Guel-Cortez, "Fastest with no-overshoot velocity control design of a two-differential robotic formation," in *Advances in Automation and Robotics Research: Proceedings of the 3rd Latin American Congress on Automation and Robotics, Monterrey, Mexico 2021*, pp. 71–79, Springer, 2021.

[10] C. Méndez-Barrios, S.-I. Niculescu, C.-I. Morarescu, and K. Gu, "On the fragility of PI controllers for time-delay SISO systems," in *2008 16th mediterranean conference on control and automation*, pp. 529–534, 2008.

[11] I.-C. Morărescu, C.-F. Méndez-Barrios, S.-I. Niculescu, and K. Gu, "Stability crossing boundaries and fragility characterization of PID controllers for SISO systems with I/O delays," in *Proceedings of the 2011 American control conference*, pp. 4988–4993, 2011.

[12] N. Bajcinca, "Computation of stable regions in PID parameter space for time-delay systems," in *Proc. of 5th IFAC workshop on time-delay systems*, 2005.